Bottom Depth Effects on Regular Surface Waves due to a Submerged Rankine Body with Attached Vertical Column

Peter Van Dyke*
Hydronautics Inc., Laurel, Md.

The role of finite-depth bottom on the amplitudes and slopes of the regular surface waves resulting from passage of a body at uniform velocity beneath an otherwise smooth surface has been considered. The velocity is restricted by the requirement that the Froude number based on bottom depth be less than unity. The first-order integral representation for these regular waves amplitudes are well known, but combinations of these integrals to produce a body with attached vertical column lead to interactions which significantly alter the character of the finite-depth bottom effect. Consideration of the simplified case of the sphere allows qualitative conclusions regarding wavelength and amplitude alterations, and also facilitates definition of near- and far-field regions. A typical first-order body-plus-vertical-column calculation shows wavelength effects similar to the sphere, but a significant interaction phenomenon at infinite bottom depth is progressively cancelled as depth decreases, implying large amplitude magnifications due to the finite depth. A check of the critical wake angle as a function of bottom depth yields the expected first-order equations, but the classical table of wake angle at various Froude numbers based on bottom depth is corrected.

Introduction

THE principal objective of the investigations summarized by this paper has been to obtain an understanding of the effect of a finite-depth bottom on the regular wave portion of the wake from a Rankine body with vertical column passing with uniform velocity beneath a smooth surface. The first-order integral representation of the regular wave with finite-depth bottom for a point source is well known; numerical evaluation for near-field results or approximate expressions in the far-field, for a general body made up of point and line source/sink combinations, however, requires extensive bookkeeping, best accomplished with the aid of a digital computer. A series of computer programs has been developed which calculates the first-order near- and far-field wave amplitudes and slopes for any body and vertical-column geometry, body velocity, and bottom depth.

A comprehensive summary of the numerous investigations of the problem of determining the wake due to a submerged body moving with constant velocity through a uniform fluid of infinite depth is presented by Yim.[1] The wake can be divided into the local disturbance, which decays exponentially with distance away from the body, and the regular wake, consisting of regular waves with an inverse square root decay. The first-order regular waves due to a point source/sink, creating a body, and a line source/sink, creating a vertical column, are considered, and these may be represented by a number of single integrals; evaluation of these integrals must be carried out numerically in the near-field close to the body, but they may be evaluated approximately at large distances from the body.

To study the finite depth effects, the numerical integration procedure developed by Yim has been generalized to the case of finite depth; in addition, a procedure of evaluation of the far-field regular wake has been developed. Results for regular wave amplitudes and slopes may be obtained for the entire field both in the plane of motion and at angles out of this plane, but within the critical wake angle; the depth is sufficiently large, however, to be such that the Froude number based on bottom depth is always less than unity. The calculation procedures are embodied in computer programs whose input is the geometry of the body formed by a point source/sink combination and a vertical column formed by a vertical line source/sink in the same vertical plane as the point source sink. In addition to the geometry and relative position and velocity of the body with vertical column, a reference point at the surface is specified, with positions given along radial lines on the surface from this point at which the wave amplitude and slope are to be evaluated.

A particular case of this general configuration occurs when the vertical column is absent and the point source and sink are coincident; this results in a spherical body, and the point source/sink becomes a horizontal dipole. Previous work by Havelock[2] has covered the derivation of the first-order integral expressions for the dipole in a finite depth fluid; Haskind[3] and Kostyukov[4] have employed similar formulations, and the latter has obtained the far-field expression for wave amplitude in the plane of motion. Consideration of the particular case of the sphere is valuable as a check on the general program, but also provides qualitative insight into the effects of bottom depth on the regular wave pattern. In particular, approximate expressions for the amplitude, slope, and wave length changes in the plane of motion, due to finite depth, are obtained.

Results for a typical body-plus-vertical-column combination are then obtained and effects of the finite bottom depth are displayed. Similarities and differences between the spheroidal and general body results are discussed.

As part of the derivation of the finite depth equations, the critical wake angle may be studied. This produces the expected equations derived by Havelock[2] and presented by several other authors. A check of the table of wake angles for various Froude numbers based on bottom depth, however, reveals inaccuracies which are corrected here.

The Equations

The usual assumptions regarding homogeneity, inviscidness, and imcompressibility of the fluid, smallness of the surface wave with regard to the wavelength, and linearity of results, allows the wave height, ζ, for a point source to be written to first-order as

$$\zeta = -(M/2\pi U)Re \int_{-\pi}^{\pi} \int_{0}^{\infty} \frac{2ik \sec\theta e^{ik\omega} \cosh[k(d-f)]}{[k - k_0 \sec^2\theta \tanh(kd) - i\mu \sec\theta] \cosh(dk)} dk d\theta \quad (1)$$

Received April 24, 1972; revision received October 24, 1972. This work was sponsored by the Applied Physics Laboratory of The Johns Hopkins University, under Contract 341717.
Index category: Vessel and Control Surface Hydrodynamics.
*Principal Research Scientist. Member AIAA.

where M is the source strength and U the constant velocity; d is the bottom depth and f the source depth in an xyz coordinate system on the surface at the source with x directed towards the rear of the body. θ and k are variables of integration, with

$$k_0 = g/U^2 \tag{2}$$

and

$$\omega = x\cos\theta + y\sin\theta = R\cos(\theta - \phi)$$

with $$R^2 = x^2 + y^2 \text{ and } \tan\phi = y/x \tag{3}$$

Consideration of second-order nonlinear effects involving interactions of the surface and bottom with the body have been ignored, since the first-order equations give solutions which illustrate the qualitative effect of the bottom on the surface waves. The artificial friction μ is a device to facilitate evaluation of the integral by contour integration, and is set to zero afterwards. The contour integration yields the two integrals for the local disturbance and regular wave; the regular wave result is

$$\zeta = (4M/Uf)\int_{-\pi/2+\phi}^{\pi/2} \frac{\tilde{k}\sec\theta\cos(\tilde{k}\omega/f)\cosh[\tilde{k}(\alpha-1)]}{[1-k_0 d\sec^2\theta\,\mathrm{sech}^2(\tilde{k}\alpha)]\cosh(\tilde{k}\alpha)}d\theta \tag{4}$$

with

$$\alpha = d/f \tag{5}$$

and

$$\tilde{k} = k_0 f\sec^2\theta\tanh(\tilde{k}\alpha) \tag{6}$$

By defining the variable t as

$$t = \tilde{k}/k_0 f\sec^2\theta \tag{7}$$

and noting that

$$Fr_d^2 = U^2/gd \tag{8}$$

Equation (6) can be simplified to

$$t = \tanh(t\sec^2\theta/Fr_d^2) \tag{9}$$

This equation has a real positive root only for

$$\sec^2\theta > Fr_d^2 \tag{10}$$

and so for the minimum value of θ equal to 0,

$$Fr_d < 1 \tag{11}$$

For comparison with the infinite depth case, Eq. (4) can be rewritten as

$$\zeta = (4Mk_0/U)\int_{-\pi/2+\phi}^{\pi/2} \frac{t\sec^3\theta\cos(k_0 t\omega\sec^2\theta)\cosh[k_0 tf\sec^2\theta(\alpha-1)]}{[1-k_0 d\sec^2\theta\,\mathrm{sech}^2(k_0 td\sec^2\theta)]\cosh(k_0 td\sec^2\theta)}d\theta \tag{12}$$

which reduces to the infinite depth case ($\alpha = \infty$, $t = 1$).

To evaluate the line source or sink, this point value must be integrated over the vertical length of the line. Employing Eq. (5), this integration can be seen to involved only the term cosh $[k_0 tf\sec^2\theta\,(\alpha - 1)]$, which becomes

$$-\sinh[k_0 tf\sec^2\theta(\alpha-1)]/tk_0\sec^2\theta \tag{13}$$

Similarly, evaluation of slopes involves only the term cos $(k_0 t\omega\sec^2\theta)$, which becomes

$$-\sin(k_0 t\omega\sec^2\theta)k_0 t\sec^2\theta\cos(\theta-\phi) \tag{14}$$

where the slope is defined as $d\zeta/dR$; that is, measured with respect to the radial line from the origin.

The strength, M, of the point source/sink system is determined from the equations (see Milne-Thomson[5])

$$\mathrm{I}(1-\epsilon_s^2)^2 = 16\epsilon_s(M/UL^2) = 4H^2/L^2[(4H^2/L^2) + \epsilon_s^2]^{1/2} \tag{15}$$

with ϵ_s the ratio of separation length to total length L, H the body radius, and U the constant velocity. The strength, m, of the line source/sink system is determined from

$$1-\epsilon_l^2 = 4\epsilon_l(m/Ul);\quad (4h^2/l^2) - \epsilon_l^2 = 4\epsilon_l(h/l)\cot[4\epsilon_l h/l(1-\epsilon_l^2)] \tag{16}$$

with ϵ_l the ratio of separation length to vertical-column length l, and h the vertical-column width. The point and line source/sink systems are illustrated in Fig. 1. For given values of H and L, and h and l, Eqs. (15) and (16) can be solved for ϵ_s, M/U, ϵ_l, and m/U; or in nondimensional form, values of H/L, h/L, and l/L, allow solution for ϵ_s, M/UL^2, ϵ_l, and m/UL.

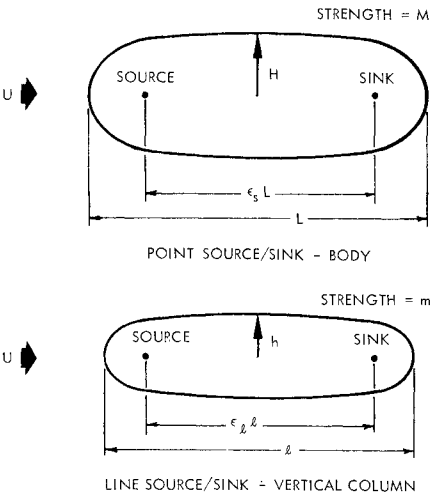

Fig. 1 Point and line source/sink modeling body and vertical column.

The Sphere

The integral for the sphere, the geometry of which is shown in Fig. 2, is derived directly from Eq. (12) by employing the definition of the horizontal dipole in terms of the point source/sink. Noting that the dipole strength is related to radius, a, by

$$M/U = a^3/2 \tag{17}$$

and performing the differentiation yields

$$\zeta = -2k_0^2 a^3\int_{-\pi/2}^{\pi/2} \frac{t^2\sec^4\theta\sin(k_0 tx\sec\theta)\cosh[k_0 tf\sec^2\theta(\alpha-1)]}{[1-k_0 d\sec^2\theta\,\mathrm{sech}^2(k_0 td\sec^2\theta)]\cosh(k_0 td\sec^2\theta)}d\theta \tag{18}$$

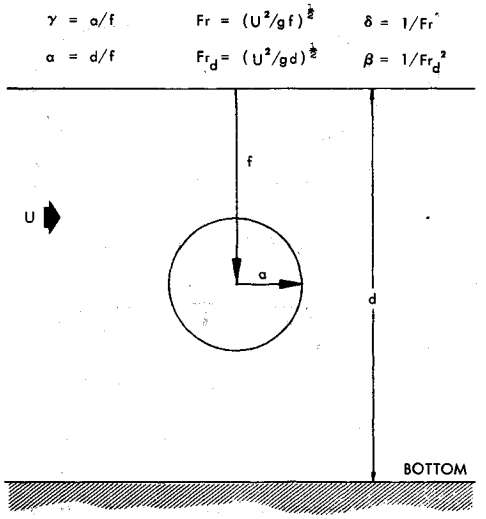

Fig. 2 Sphere geometry.

where only the plane of motion ($\phi = 0$, $\omega = x \cos\theta$) is being considered.

It is convenient to express the amplitude in dimensionless form by defining

$$\xi = \zeta/L \quad \gamma = a/f \quad Fr^2 = U^2/gf \quad W = k_0 R/2\pi \tag{19}$$

with

$$L = 2a \quad \beta = 1/Fr_d^2 \quad \delta = 1/Fr^2 \tag{20}$$

Equation (18) then becomes

$$\xi = -(\gamma\delta)^2 \int_{-\pi/2}^{\pi/2} \frac{t^2 \sec^4\theta \sin(2\pi Wt \sec\theta)\cosh[\delta t \sec^2\theta(\alpha - 1)]}{[1 - \beta \sec^2\theta \operatorname{sech}^2(\beta t \sec^2\theta)]\cosh(\beta t \sec^2\theta)} d\theta \tag{21}$$

By considering this as an integral of the type

$$I = \int F(\theta) \sin[xg(\theta)]d\theta \tag{22}$$

the asymptotic approximation for large x can be written

$$I \sim \left[\frac{2\pi}{|xg''(\theta_0)|}\right]^{1/2} F(\theta_0) \sin[xg(\theta_0) \pm \pi/4] \tag{23}$$

where the sign on $\pi/4$ is selected by

$$g''(\theta_0) > 0, \quad + \pi/4 \tag{24}$$

The asymptotic solution for Eq. (21) is then

$$\xi = -\frac{(\gamma\delta t)^2 \cosh[\delta t(\alpha - 1)] \sin(2\pi Wt + \pi/4)}{\cosh(\beta t)(1 - \beta^2 \operatorname{sech}^4\beta t)^{1/2}(Wt)^{1/2}} \tag{25}$$

with

$$t = \tanh\beta t \tag{26}$$

which agrees with the result given by Kostyukov.[4] For the infinite depth case, this reduces to the result

$$\xi = -\frac{(\gamma\delta)^2 e^{-\delta} \sin(2\pi W + \pi/4)}{(W)^{1/2}} \tag{27}$$

The asymptotic expression for the wave slope can be written directly, either by differentiating Eq. (21) and evaluating the integral, or by direct differentiation of Eq. (25), to yield

$$\frac{d\zeta}{dx} = -\frac{2(\gamma\delta t)^3 \cosh[\delta t(\alpha - 1)] \cos(2\pi Wt + \pi/4)}{\cosh\beta t(1 - \beta^2 \operatorname{sech}^4\beta t)^{1/2}(Wt)^{1/2}} \tag{28}$$

and

$$\frac{d\zeta}{dx} = -\frac{2(\gamma\delta)^3 e^{-\delta} \cos(2\pi W + \pi/4)}{(W)^{1/2}} \tag{29}$$

for the infinite depth case.

Near-field results may be obtained by a direct numerical integration of Eq. (21); this was carried out using a straightforward Simpson's rule integration scheme.

The first results were obtained for the near-field, infinite depth problem; the results for wave amplitude at the first maximum point are shown in Fig. 3. From these results it can be seen that the point of maximum amplitude occurs at a constant Fr value, and this maximum is proportional to γ^2. Inspection of Eq. (27) yields similar results in the far-field, with maximum values at Fr of $(2/3)^{1/2}$ proportional to γ^2.

Next, the specific case of a sphere with $\gamma = 0.5$ is considered. Results for the near- and far-field are shown in Fig. 4. At each Fr value, the bottom is brought up almost to the sphere, increasing the Fr_d value to nearly the theoretical maximum

$$Fr_{d_{max}} = Fr/(1 + \gamma)^{1/2} \tag{30}$$

The range of applicability of the near-field results varies as a function of Fr, decreasing as Fr increases; the far-field results extend generally to a value of W near 1. The calculations confirm that the effects of the finite bottom are not felt at Fr_d below 0.5. The effects of the bottom are most noticeable in the increased wave length in the far-

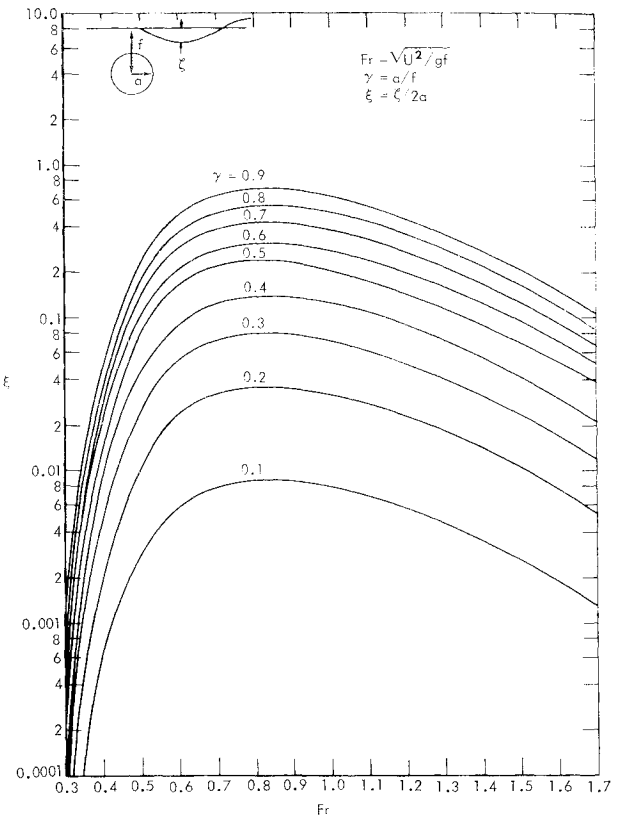

Fig. 3 Near-field infinite depth solution for the sphere.

field; the amplitude is also increased, but this effect seems to peak at $Fr \sim 0.8$, and decreases at higher Fr. At Fr of 1.1, an additional Fr_d is plotted, showing that the amplitude increase depends primarily on Fr and Fr_d. The near-field results, however, are of different character; the position of maximum amplitude changes, but the amplitude magnification is also significant at all Fr.

Approximate expressions for these bottom effects on wave length and amplitude in the far-field can be derived from Eq. (25), using the approximate solution to Eq. (26),

$$t = 1 - Fr_d^{9.03} \tag{31}$$

which is accurate up to a Fr_d of 0.8. From Eq. (25), the wave length increases by

$$1/t = 1/(1 - Fr_d^{9.03}) \tag{32}$$

The amplitude increase may be approximated by

$$(1 - Fr_d^{9.03})^{3/2}(e^{\delta\, Fr_d^{9.03}})/(1 - 4Fr_d^{14.06})^{1/2} \tag{33}$$

which can be written

$$1 + [(\delta - 3/2) + 2Fr_d^{5.03}]Fr_d^{9.03} \tag{34}$$

The finite bottom behavior illustrated in Fig. 4 can be confirmed with these approximate expressions: the wave length increases are accurately described by Eq. (32); the amplitude magnification for $Fr = 1.1$ ($\delta = 0.826$) for Fr_d of 0.74 and 0.87 is described by Eq. (34); and, the peaking of the amplitude magnification for the Fr_d near the maximum (obtained with $\alpha = 1.6$ for all Fr) can be obtained by employing the relationship

$$\beta = \alpha\delta \tag{35}$$

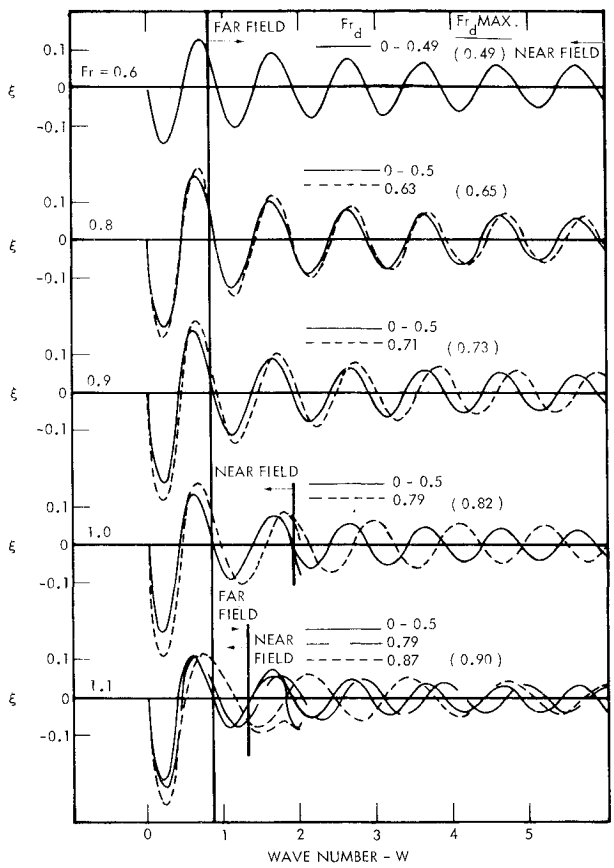

Fig. 4 Regular waves on centerline for sphere with $\gamma = 0.5$.

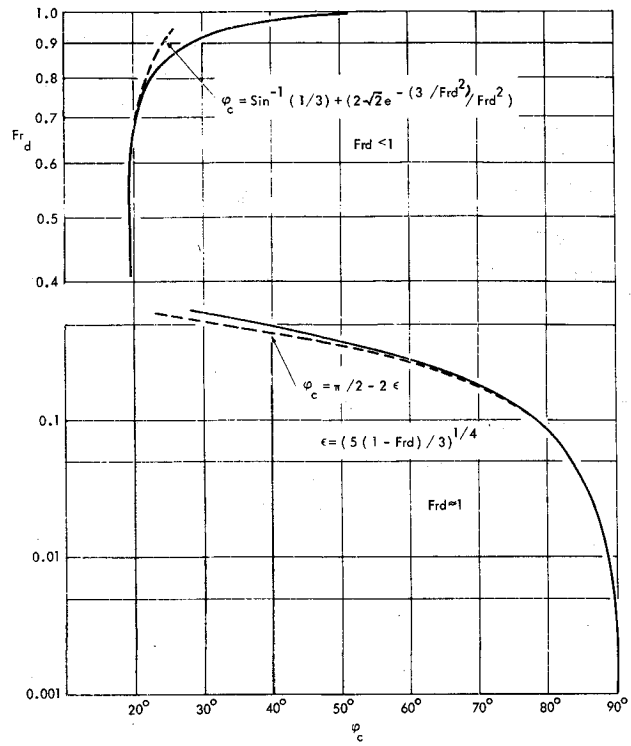

Fig. 5 Critical wake angles.

and rewriting Eq. (34) as

$$1 + [(\delta - 3/2) + 2(\alpha\delta)^{-2.515}](\alpha\delta)^{-4.515} \tag{36}$$

Now, the maximum of this expression occurs, for α of 1.6, at a δ of 1.54 or Fr of 0.81.

The slope magnification factor can be determined by noting, in Eqs. (28) and (29), that only an additional factor of t is present compared to the amplitude factor from Eqs. (25) and (27). The slope factor, comparable to Eq. (34), is then

$$1 + [(\delta - 5/2) + 2Fr_d^{5.03}]Fr_d^{9.03} \tag{37}$$

An analysis similar to that carried out for amplitude indicates a maximum slope magnification at Fr of 0.56 for the sphere with α of 1.6 and γ of 0.5.

The General Body

The analysis of the general body with attached vertical column involves the separate evaluation of the four components representing the point source, point sink, line source, and line sink.

In the near field, this evaluation is carried out using Gauss and Laguerre polynomials following the procedures outlined by Yim. In the far field, the integral of Eq. (12) is evaluated asymptotically as outlined in the previous section for the sphere. There are, however, a few complexities.

The asymptotic result is given by the sum of two expressions of the form of Eq. (23), with cos replacing sin, where

$$g(\theta) = R\rho t \cos(\theta - \phi)/d \tag{38}$$

and with t given by

$$t = \tanh(\rho t) \tag{39}$$

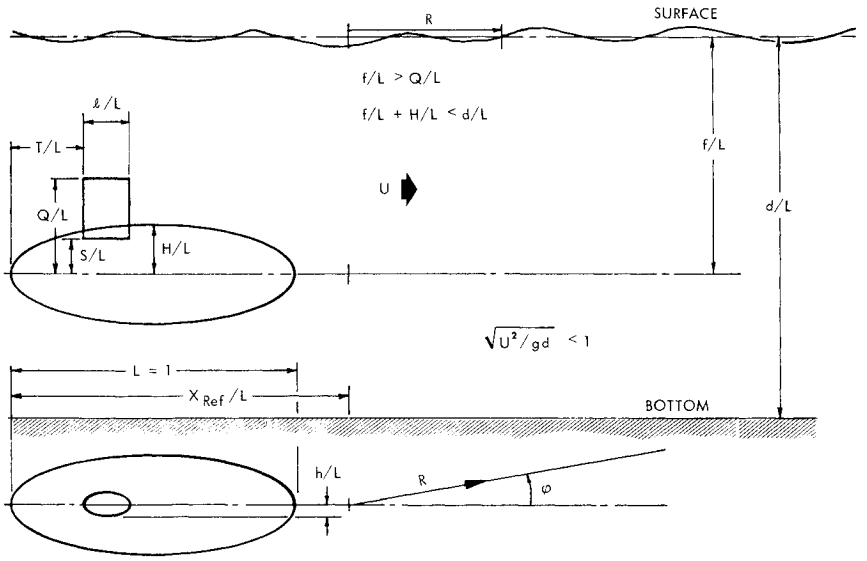

Fig. 6 Geometry of general body.

where

$$\rho = \beta \sec^2\theta \tag{40}$$

The function $F(\theta)$ is

$$F(\theta) = \frac{4k_0L(M/UL^2)t \sec^3\theta \cosh[\delta t \sec^2\theta(\alpha - 1)]}{[1 - \rho \operatorname{sech}^2(\rho t)] \cosh(\rho t)} \tag{41}$$

where the resulting amplitude is normalized by the overall body (point source/sink) length L. The point θ_0 results from

$$g'(\theta_0) = 0 \tag{42}$$

where

$$g'(\theta) = R[2\rho t \tan\theta(1 + P) \cos(\theta - \phi) - \rho t \sin(\theta - \phi)]/d \tag{43}$$

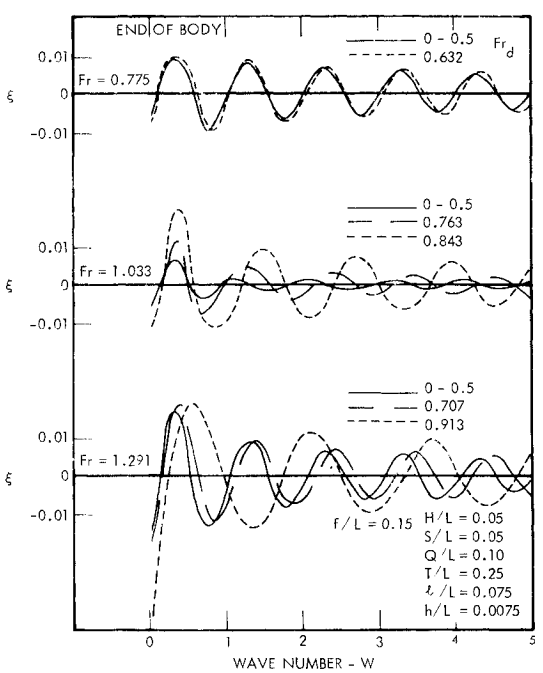

Fig. 7 Regular waves on centerline for general body.

with

$$P = \rho \operatorname{sech}^2\rho t/(1 - \rho \operatorname{sech}^2\rho t) \tag{44}$$

Two distinct values of θ_0, θ_1 and θ_2, are then determined from

$$2(1 + P) \tan^2\theta + (1 + 2P) \cot\phi \tan\theta + 1 = 0 \tag{45}$$

With $P = 0$ for infinite depth, the result given by Yim is obtained. There are real solutions to the equation only at values of ϕ within the critical wake angle. This critical angle for various depths is obtained through solution of Eqs. (39, 40, 44, and 45). This should be done not by specifying a value of β, in which case an iterative solution is required, but by picking a value of ρ, solving for t and P, finding the angle θ_0 at which θ_1 equals θ_2 from Eq. (45), and finally solving Eq. (40) for β. This latter method yields the classical Havelock equations when ρt, β, P, and $1/\rho$ are equated to kh, P, $N/1\text{-}N$, and M of Ref. 2.

By carrying out these calculations, large inaccuracies were found in the table of values of critical angle for various Fr_d given in Ref. 2. Figure 5 presents a corrected picture of the wake angle, where the limiting value

$$\phi_c = \pi/2 - 2\epsilon$$

with

$$\epsilon = [5(1 - Fr_d)/3.]^{1/4}$$

holds for small ϵ, and

$$\phi_c = \sin^{-1}(1/3) + [2(2)^{1/2}e^{-(3/Fr_d^2)}]Fr_d^2$$

Table 1 Corrected critical wake angles[a]

ρt	β	ϕc	Fr_d
10	6.6667	19.4712	0.3873
8	5.3333	19.4713	0.4330
6	4.0002	19.4752	0.5000
5	3.3346	19.4958	0.5476
4	2.6732	19.6165	0.6116
3	2.0301	20.2847	0.7018
2	1.4541	23.6922	0.8293
1	1.0725	39.3173	0.9656
0.5	1.0069	59.4583	0.9966
0.2	1.0002	76.9469	0.9999
0	1.0000	90.0000	1.0000

[a]Corrections to Table III, pg. 31, Ref. 2.

is accurate for values of $Fr_d < 0.7$. A corrected table of values corresponding to those in Ref. 2 is presented as Table 1.

At a ϕ of zero, with $0 \leq P < \infty$, a value of zero for θ_1 is the only root leading to a result, and there is therefore only a single term in the solution.

Once θ_1 and θ_2 are determined, the values of $g''(\theta_0)$ are obtained from

$$g''(\theta) = R\cos(\theta - \phi)\rho t[1 + 2P - 2\tan^2\theta(1 + P) - 8\rho t^2\tan^2\theta P(1 + P)^2]/d \qquad (46)$$

For ease in assessing the numerical results, only results at $\phi = 0$ are considered. This implies a solution to Eq. (45) of $\phi = 0$, leading to a simplified form for Eq. (46).

The required geometric input to determine strengths and fix the relative positions of the sources and sinks is shown in Fig. 6. All lengths are expressed as fractions of the point source/sink body length L. The required geometry includes: body width ratio H/L; vertical column bottom and top positions relative to body, S/L and Q/L; vertical column longitudinal position relative to body T/L; vertical column length ratio l/L; and vertical column width ratio h/L. Additional required input includes: depth ratio of body centerline f/L; bottom depth ratio d/L; velocity and length of body, U and L, or a Froude number based on body length, body depth (Fr) or bottom depth (Fr_d); the reference length ratio X_{ref}/L to the reference point; and the radial distance R and angle from centerline ϕ from the reference point to the point where the wave character is to be determined.

Figure 7 presents some results for the regular wave on the centerline for a general body with f/L of 0.15, H/L and S/L of 0.05, Q/L of 0.10, T/L of 0.25, l/L of 0.075, h/L of 0.0075, and X_{ref}/L of 1.0. The results are given for three values of Fr and for various values of Fr_d; the wave position on the centerline is characterized by the wave

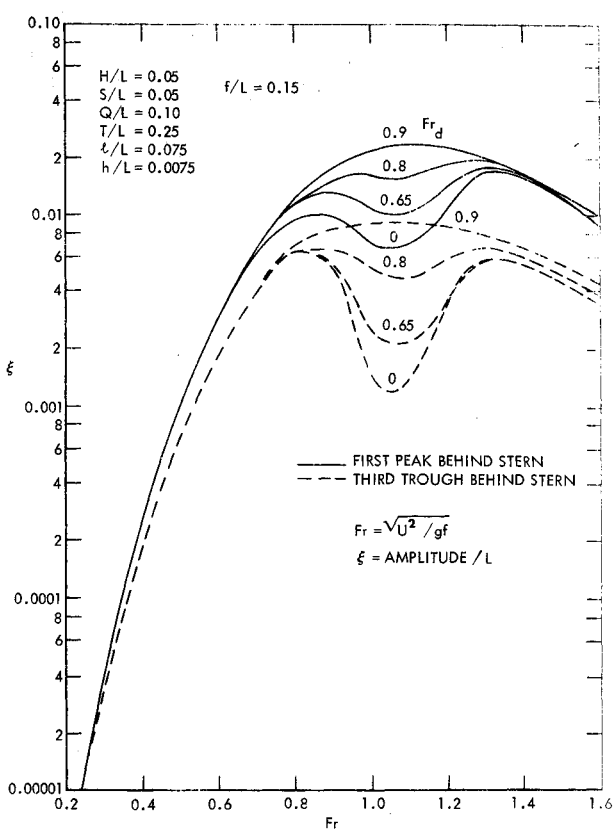

Fig. 8 Amplitude of regular waves on the centerline.

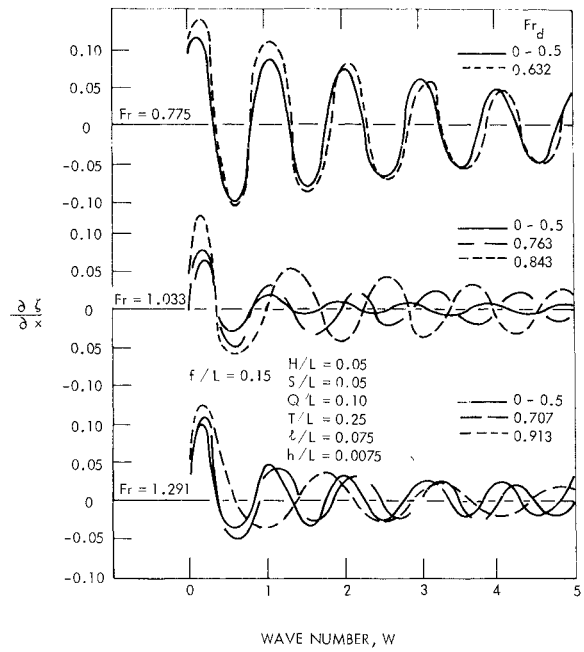

Fig. 9 Regular wave slopes on centerline for general body.

number W given by Eq. (19). These results are generally similar to those for the spherical body: an increase in Fr_d causes an amplification and wavelength increase of the regular centerline wave. The wavelength increase follows the approximate Eq. (32) up to Fr_d of about 0.8 as in the spherical case. The amplitude magnification, however, does not follow the simplified spherical amplification, primarily because of the occurrence of a significant dip in the wave amplitude at a Fr of about 1.0. This is shown in Fig. 8, where the amplitudes of the first wave peak and third wave trough behind the stern of the body are presented for increasing Fr and varying values of Fr_d. At Fr of 1.0, where the infinite-depth wave amplitude decreases significantly, the bottom effects tend to return the wave to what would be expected from a smooth amplitude vs Fr

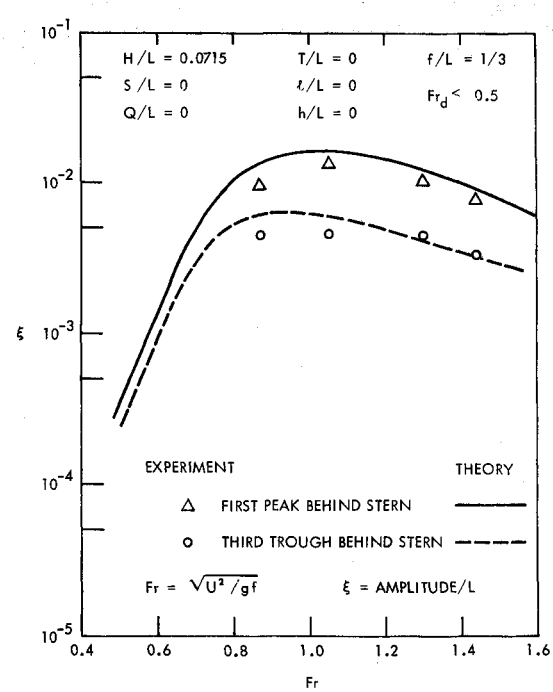

Fig. 10 Comparison of theoretical and experimental centerline wave amplitudes at varying Fr.

curve as for the sphere (Fig. 3). This produces amplification factors of as much as 4 in the near-field and 8 in the far-field. At Fr of 1.3, the amplitudes have returned to the case where bottom effects cause a moderate amplification.

Figure 9 presents the values of the slope of the regular wave on the centerline for the waves presented in Fig. 6: at low Fr, the slopes are larger (due to shorter wavelength) and the amplifications positive; at $Fr \approx 1.0$, the slope magnification is significant because of the large amplitude increases; at high Fr, the small amplitude magnification and large wavelength increase combine to produce a slope decrease with increasing Fr_d. This can be seen by considering Eq. (37), where increasing Fr decreases δ, and the 5/2 factor predominates over the 2 $Fr_d^{5.03}$ term. The slope wavelength must, of course, follow the amplitude wavelength, and so is described approximately by Eq. (32) for Fr_d below 0.8. The decay characteristics of the amplitude and slope results of Figs. 7 and 9 are similar to the sphere: periodic in Wt with $(Wt)^{-1/2}$ decay.

Discussion

The effects of the finite-depth bottom are felt only at Fr_d above 0.5, and this implies a high Fr with an associated reduction of the region of overlap between the near-field and far-field results. The results presented by Yim are at low enough Fr so that the near-field calculation extends a significant distance behind the body. The desire to show finite-depth bottom effects in the present work, however, has brought the asymptotic analysis to the fore. The wave amplifications in the near- and far-field are different, but cannot be studied in too much detail because of the limited range of the near-field calculations and the approximate nature of the transition area. The significance of the near-field amplification results at high Fr is further confused by the fact that the local disturbance is important in the limited range of these calculations.

Exhaustive calculations for general bodies have not been carried out; rather, the general qualitative effects of the finite-depth bottom have been sought. Certainly the significant amplitude alteration at Fr of 1.0 for the example body is worthy of further study. Also, the relative importance of the body compared with the vertical column appendage in the general body calculations should be studied. For the example body selected here, the vertical column is important at low Fr due to its proximity to the surface, but the body effects dominate at high Fr due to the large body size relative to the vertical column.

Calculations of the waves off the centerline have also been neglected to date. The extensive studies of the off-centerline wake, and the situation as the critical angle is approached, are summarized by Yim. The important conclusions for the infinite-depth case are that an amplitude decrease off-centerline takes place, but a local increase, always to values less than the centerline amplitudes and slightly within the critical angle, is also characteristic. A detailed study of the effects of finite bottom depth on the off-centerline waves would be valuable to reveal the general applicability of these conclusions.

The agreement between theoretically and experimentally determined submerged body surface waves, where effects caused by proximity of the bottom are absent, are summarized in Ref. 6. The agreement between the experiment and theory for the total wake is exceptional. The experimental data presented in Ref. 6 clearly demonstrate the peaking of regular wave amplitudes at $Fr \approx 1.0$, as shown in Fig. 10. There are no available experimental data on the finite-depth bottom influence on surface waves, so the particular effects studied here are, as yet, unverified.

References

[1]Yim, B., "Waves Due to a Submerged Body," TR 231-3, May 1963, Hydronautics Inc., Laurel, Md.

[2]Havelock, T. H., "Wave Resistance," *The Collected Papers of Sir Thomas Havelock on Hydrodynamics,* edited by C. Wigley, ONR/ACR-103, Office of Naval Research, March 1965, pp. 278–287; also "The Propagation of Groups of Waves in Dispersive Media with Application to Waves on Water Produced by a Travelling Disturbance," pp. 1–33.

[3]Haskind, M. D., "On the Translational Motion of Bodies Under the Free Surface of a Heavy Fluid of Finite Depth," *Prikladnia Mathematica i Mekhanika,* Vol. IX, No. 1, 1945; also "General Theory of Waves Resistance for Body Motion in a Fluid of Finite Depth," *Prikladnia Mathematica i Medkhanika,* Vol. IX, No. 3, 1945.

[4]Kostyukov, A. A., "Wave Formation by a Ship Underway," *Theory of Ship Waves and Wave Resistance,* edited by L. Landweber and J. N. Newman, E.C.I., Iowa City, Iowa, 1968, pp. 165, 148.

[5]Milne-Thomson, L. M., *Theoretical Hydrodynamics,* 4th ed., MacMillan, New York, 1960, pp. 206, 461.

[6]Hsu, C. C. and Yim, B., "A Comparison Between Theoretical and Measured Waves Above a Submerged Rankine Body," TR 231-10, Feb. 1966, Hydronautics Inc., Laurel, Md.